



# Cancer Research

## Cyclin E1 Deregulation Occurs Early in Secretory Cell Transformation to Promote Formation of Fallopian Tube–Derived High-Grade Serous Ovarian Cancers

Alison M. Karst, Paul M. Jones, Natalie Vena, et al.

*Cancer Res* 2014;74:1141-1152. Published OnlineFirst December 23, 2013.

**Updated version** Access the most recent version of this article at:  
doi:[10.1158/0008-5472.CAN-13-2247](https://doi.org/10.1158/0008-5472.CAN-13-2247)

**Supplementary Material** Access the most recent supplemental material at:  
<http://cancerres.aacrjournals.org/content/suppl/2013/12/23/0008-5472.CAN-13-2247.DC1.html>

**Cited Articles** This article cites by 47 articles, 12 of which you can access for free at:  
<http://cancerres.aacrjournals.org/content/74/4/1141.full.html#ref-list-1>

**E-mail alerts** [Sign up to receive free email-alerts](#) related to this article or journal.

**Reprints and Subscriptions** To order reprints of this article or to subscribe to the journal, contact the AACR Publications Department at [pubs@aacr.org](mailto:pubs@aacr.org).

**Permissions** To request permission to re-use all or part of this article, contact the AACR Publications Department at [permissions@aacr.org](mailto:permissions@aacr.org).

## Cyclin E1 Deregulation Occurs Early in Secretory Cell Transformation to Promote Formation of Fallopian Tube-Derived High-Grade Serous Ovarian Cancers

Alison M. Karst<sup>1,3</sup>, Paul M. Jones<sup>1</sup>, Natalie Vena<sup>1,2</sup>, Azra H. Ligon<sup>2,3,4</sup>, Joyce F. Liu<sup>1,3</sup>, Michelle S. Hirsch<sup>3,5</sup>, Dariush Etemadmoghadam<sup>6,7,8</sup>, David D.L. Bowtell<sup>6,7,8,9</sup>, and Ronny Drapkin<sup>1,3,5</sup>

### Abstract

The fallopian tube is now generally considered the dominant site of origin for high-grade serous ovarian carcinoma. However, the molecular pathogenesis of fallopian tube-derived serous carcinomas is poorly understood and there are few experimental studies examining the transformation of human fallopian tube cells. Prompted by recent genomic analyses that identified cyclin E1 (*CCNE1*) gene amplification as a candidate oncogenic driver in high-grade serous ovarian carcinoma, we evaluated the functional role of cyclin E1 in serous carcinogenesis. Cyclin E1 was expressed in early- and late-stage human tumor samples. In primary human fallopian tube secretory epithelial cells, cyclin E1 expression imparted malignant characteristics to untransformed cells if p53 was compromised, promoting an accumulation of DNA damage and altered transcription of DNA damage response genes related to DNA replication stress. Together, our findings corroborate the hypothesis that cyclin E1 dysregulation acts to drive malignant transformation in fallopian tube secretory cells that are the site of origin of high-grade serous ovarian carcinomas. *Cancer Res*; 74(4); 1141–52. ©2013 AACR.

### Introduction

High-grade serous ovarian carcinoma (HGSOC) is a devastating disease responsible for the deaths of approximately 125,000 women worldwide each year (1). The vast majority of patients die within 5 years of being diagnosed. Poor survival rates reflect the difficulty of early detection and the lack of effective treatments for advanced-stage disease. Although the pathogenesis of HGSOC is poorly understood, recent years have witnessed significant progress in uncovering its origins. Mounting molecular genetic evidence suggests that most high-grade serous tumors involving the ovary likely arise from the fallopian tube epithelium rather than the ovarian surface epithelium (2). Over half of the patients with HGSOC have early-stage noninvasive lesions called serous tubal intraepithelial carcinoma (STIC) in their fallopian tubes. HGSOC and STIC are not only histologically similar, but they often harbor identical gene mutations and molecular profiles, strongly

suggesting a clonal relationship (2–4). The genomic landscape of HGSOC is dominated by two main features: (i) ubiquitous somatic *TP53* (tumor protein p53) mutations and (ii) numerous DNA amplifications and deletions (5, 6). *TP53* mutation is an early event and has been found in benign-appearing putative precursor lesions within the fallopian tube epithelium called "p53 signatures" (3). A third important genomic feature of HGSOC is the presence of germline *BRCA1* (breast cancer 1, early onset) or *BRCA2* (breast cancer 2, early onset) mutations in approximately 23% of patients, which is the predominant genetic risk factor for HGSOC (5). BRCA proteins maintain genomic stability by participating in homologous recombination repair of DNA double-strand breaks (DSB). Approximately 50% of HGSOC cases exhibit defects in homologous recombination pathway components, causing chromosomal instability (5). In the remaining 50% of cases, however, the driving force behind chromosomal instability remains unclear (7). One possible driver is *CCNE1* (cyclin E1), a gene that is recurrently amplified and/or overexpressed in HGSOC. Cyclin E1 is involved in G<sub>1</sub>–S phase cell-cycle progression and centrosome amplification. During the cell cycle, it complexes with cyclin-dependent kinase 2 (CDK2) to promote E2F transcription factor 1 activation and S-phase entry (8). Constitutive cyclin E1 expression has been shown to cause chromosomal instability in both primary human cells and mice (9–11). Interestingly, *CCNE1* amplifications are mutually exclusive with *BRCA1/BRCA2* mutations in HGSOC, suggesting that their respective impacts on genomic stability are either redundant or synthetically lethal (7). Unlike *BRCA1/BRCA2*-mutant tumors, which initially respond to platinum-based chemotherapy, *CCNE1*-amplified tumors are associated with primary platinum failure (12–14). Given the lack of treatment options

**Authors' Affiliations:** <sup>1</sup>Department of Medical Oncology; <sup>2</sup>Center for Molecular Oncologic Pathology, Dana-Farber Cancer Institute; <sup>3</sup>Harvard Medical School; <sup>4</sup>Department of Pathology, Division of Cytogenetics; <sup>5</sup>Department of Pathology, Division of Women's and Perinatal Pathology, Brigham and Women's Hospital, Boston, Massachusetts; <sup>6</sup>Peter MacCallum Cancer Centre, East Melbourne; <sup>7</sup>Department of Oncology, Peter MacCallum Cancer Centre; Departments of <sup>8</sup>Pathology and <sup>9</sup>Biochemistry and Molecular Biology, University of Melbourne, Melbourne, Victoria, Australia

**Corresponding Author:** Ronny Drapkin, Dana-Farber Cancer Institute, Jimmy Fund Building, Room 215D, 450 Brookline Avenue, MA 02215. Phone: 617-632-4380; Fax: 617-582-8761; E-mail: ronny\_drapkin@dfci.harvard.edu

doi: 10.1158/0008-5472.CAN-13-2247

©2013 American Association for Cancer Research.

for these patients, it is important that we interrogate the mechanisms by which *CCNE1* contributes to HGSOC initiation, progression, and drug resistance to identify potential therapeutic targets. Here, we examine the oncogenic role of *CCNE1* in HGSOC development, first by characterizing its expression in early- and late-stage tumors, and secondly by generating an *in vitro* model of cyclin E1-mediated transformation using primary human fallopian tube secretory epithelial cells (FTSEC). We show that constitutive cyclin E1 expression imparts malignant characteristics to untransformed but p53-compromised FTSECs, accompanied by accumulation of DNA damage and altered transcription of DNA damage response (DDR) genes related to replication stress.

## Materials and Methods

All methods involving human tissue were approved by the Institutional Review Boards of Brigham and Women's Hospital (BWH; Boston, MA) and Dana-Farber Cancer Institute (Boston, MA).

### Tissue microarray

A tissue microarray (TMA) containing 140 primary high-grade, International Federation of Gynecology and Obstetrics (FIGO) stage III–IV serous ovarian adenocarcinoma samples, from patients who underwent cytoreductive surgery during 1999 to 2005, was obtained from the Department of Pathology, BWH (15).

### FISH analysis of TMA

Two human bacterial artificial chromosome clones, purchased from the Children's Hospital Research Institute, were cohybridized: (i) a *CCNE1* probe RP11-345J21 (red signal) mapping to 19q12 and including *CCNE1*, *PLEKHFI1*, and *CI9orf12*, and (ii) a chromosome 19 reference probe RP11-81M8 (green signal) mapping to 19p13.3. TMA sections and probes were codenatured, hybridized, and counterstained with 4',6-diamidino-2-phenylindole (DAPI) as described in the Supplementary Materials and Methods. Images were captured using an Olympus BX51 fluorescent microscope running Cyto-Vision Genus v3.9 software (Applied Imaging). Tumors were classified by *CCNE1* copy number as follows: (i) samples with two copies of the *CCNE1* probe and two copies of the reference probe were considered disomic for *CCNE1*; (ii) samples with a *CCNE1*: control probe ratio of >1 but <3 were considered to have relative *CCNE1* gain; (iii) samples with a *CCNE1*: control probe ratio of 1 but greater than two copies of each probe were considered polysomic; and (iv) samples with a *CCNE1*: control probe ratio of  $\geq 3$  were considered amplified. Spatial organization of *CCNE1* signals was also considered in assigning samples to the amplified group (e.g., clustering of *CCNE1* signals around a single control probe).

### Immunohistochemical analysis of TMA

Immunohistochemical (IHC) staining for cyclin E1 was carried out using the Envision Plus/Horseradish Peroxidase System (Dako). Antibody conditions are specified in Supplementary Table S1. Stained cores were evaluated by two independent observers (including a histopathologist) and scored by

the percentage of immunopositive tumor cells present: 0 = <10%, 1 = 10% to 25%, 2 = 25% to 50%, 3 = 50% to 75%, and 4 = >75%. When scores differed between replicate cores, the highest score was used.

### IHC analysis of fallopian tubes

Fourteen cases of high-grade pelvic serous carcinoma were retrieved from the BWH Department of Pathology 2008 to 2011 archives. Serial tissue sections were immunostained for p53, Ki-67, and cyclin E1 (see Supplementary Table S1), and then evaluated for the presence of early lesions. p53 signature was defined as  $\geq 12$  consecutive p53-positive secretory cells with normal morphology and low Ki-67 expression (<10% positive nuclei; ref. 16). Tubal intraepithelial lesion in transition (TILT) was defined as  $\geq 12$  consecutive p53-positive secretory cells with mild cytologic atypia and/or moderately elevated Ki-67 expression (10%–50% positive nuclei; ref. 17). Both p53 signatures and TILTs were classified as putative precursor lesions. STIC was defined as a region of secretory cells exhibiting significant nuclear atypia, loss of polarity, and high Ki-67 expression (>50% positive nuclei). Cyclin E1 expression was scored as negative (<10% positive cells), low (10%–50% positive cells), or high (>50% positive cells). If more than one STIC was present within a single case, each lesion was evaluated separately and the highest score was used.

### Cell lines

The FT282 cell line was established from fresh normal human fallopian tube tissue obtained from the BWH Department of Pathology on March 14, 2011. Epithelial cells were enzymatically dissociated, plated, and transduced with viral vectors using methods recently described (18, 19). Vectors expressing human telomerase reverse transcriptase (TERT; pBABE-hygro-TERT; ref. 20) and mutant p53<sup>R175H</sup> (pLenti6/V5-TP53<sup>R175H</sup>; ref. 21) were obtained from Addgene. Derivative cell lines (FT282-V, FT282-CCNE1) were generated using pMSCV-neo-(empty) and pMSCV-neo-*CCNE1*, encoding full-length *CCNE1* subcloned from pRc/CMV 7946. Plasmids were validated by sequencing. Cells were characterized by short tandem repeat (STR) analysis using the Promega Cell ID System (cat. no. G9500) on August 6, 2013. Their STR profile was consistent over multiple passages and did not match any established cell lines.

### Western blot analysis

Cell lysates were analyzed by SDS-PAGE, blotted onto nitrocellulose membranes, then incubated with primary antibody overnight at 4°C, followed by HRP-conjugated secondary antibody for 1 hour. Protein bands were visualized using a FluorChem HD2 imager (Cell Biosciences). See Supplementary Materials and Methods for additional details.

### Sulforhodamine B assay

Cells were seeded in 96-well plates (10<sup>3</sup> cells per well, 12 replicates) and fixed every 24 hours with 10% trichloroacetic acid. Fixed cells were stained with 0.12% sulforhodamine B (SRB)/1% glacial acetic acid for 30 minutes and destained with 1% acetic acid. Cell density was quantified by adding 10 mmol/L

Tris base (100  $\mu$ L/well) and measuring absorbance at 560 nm using a Modulus Microplate Reader (Turner Biosystems).

#### Clonogenic assay

Cells were seeded in 6-well plates (500 cells per well, triplicate wells). Ten days later, colonies were fixed with 10% buffered formalin, stained with 0.5% crystal violet, and counted.

#### Anchorage-independent growth assay

Cells were suspended in 0.6% noble agar and seeded over a 0.8% agar base in 6-well plates ( $5 \times 10^3$  cells per well, triplicate wells). Six weeks later, colonies were stained with 0.05% crystal violet. Six microscopic fields per well were photographed ( $\times 20$  magnification) and the number of colonies  $>0.1$  mm was counted.

#### $\gamma$ -H2AX immunofluorescent staining

Cells grown on glass cover slips were fixed with 4% paraformaldehyde/PBS, permeabilized with 0.5% Triton X-100/PBS, and blocked with SuperBlock buffer (Pierce). Primary p-H2A.X Ser139 antibody (see Supplementary Table S1) was applied overnight at 4°C, followed by rhodamine-conjugated secondary antibody for 1 hour. Cover slips were mounted onto glass slides using DAPI-containing medium. Images were acquired using an Olympus BX51 fluorescence microscope with attached DP71 camera and DP Manager software. Four microscopic fields/slides were photographed ( $\times 40$ ) and nuclei with prominent foci were counted.

#### Comet assay

The Comet Assay Kit (Trevigen) was used according to the manufacturer's instructions. Briefly, cells were suspended in agarose, layered onto slides (500 cells per slide), lysed, and subjected to electrophoresis (1 V/cm) under alkaline conditions. Samples were then fixed, dried, and stained with SYBR Gold. Images were acquired as described for  $\gamma$ -H2AX staining. Comet tail size was quantified using CometScore v1.5.2.6 software (Tritek Corp.).

#### Quantitative PCR profiling

Total cellular RNA was analyzed for the expression of 84 DDR genes using Qiagen RT<sup>2</sup> Profiler PCR Arrays (cat. no. PAHS-029Z). Arrays were run in triplicate (500 ng RNA per array) using an Eppendorf Mastercycler ep Realplex thermal cycler. Data were analyzed using RT<sup>2</sup> Profiler Analysis software (Qiagen). *ACTB* (actin,  $\beta$ ) and *RPLP0* (ribosomal protein, large, P0) expressions were used to normalize data.

## Results

### *CCNE1* amplifications characterize a subset of HGSOC cases

To determine the frequency of somatic *CCNE1* amplifications in HGSOC, we queried The Cancer Genome Atlas (TCGA) database, which contains clinically annotated genomic data from 489 HGSOC samples (5). Datasets were analyzed using the Memorial Sloan-Kettering Cancer Center cBio Cancer Genomics Portal (<http://www.cbioportal.org/public-portal/index.do>; ref. 22). Somatic copy number was determined by Genomic

Identification of Significant Targets in Cancer analysis as previously described (22, 23). Our analysis revealed *CCNE1* alterations in 319 of 489 cases, including 106 cases (21.7%) of amplification, 165 cases (33.7%) of copy number gain, and 48 cases (9.8%) of heterozygous loss (Fig. 1A). Consistent with previous reports (14, 24), *CCNE1* amplifications were associated with reduced overall patient survival, determined by Kaplan-Meier analysis ( $P = 0.021148$ , log-rank test; Fig. 1B).

We next examined the mRNA data for these cases. As shown in Fig. 1C, *CCNE1* mRNA levels tended to increase with copy number. Using a Z score threshold of +1.5 to define upregulation, we found that *CCNE1* mRNA was upregulated in 90 of 489 cases (18.4%) and associated with reduced overall survival ( $P = 0.004348$ , log-rank test; Fig. 1D). Finally, we examined the protein expression data generated by reverse phase protein array (RPPA) analysis. We found that cyclin E1 was overexpressed ( $Z > 1.5$ ) in 30 of 412 cases (7.1%) and, again, was strongly associated with reduced overall survival ( $P = 0.001016$ , log-rank test; Fig. 1E).

In just over half of amplified cases (56.6%; 60 of 106), amplification resulted in mRNA upregulation, and conversely, two thirds (66.7%; 60 of 90) of tumors with high mRNA levels had an underlying amplification. Correlation with protein expression, however, was lower. Although high cyclin E1 protein levels could be attributed to *CCNE1* amplification in 63.3% (19 of 30) of cases, only 24.4% (19 of 78) of amplified cases actually overexpressed cyclin E1 protein. This seems surprisingly low and might be an underestimate due to the fact that RPPA data were available for only 78 amplified cases. Amplification without corresponding expression might indicate that amplified *CCNE1* is not always constitutively transcribed or that transcription is countered by posttranscriptional repression, perhaps by microRNAs (25). Alternatively, low cyclin E1 protein expression could reflect increased rates of ubiquitin-mediated degradation.

### *CCNE1* amplification is associated with increased cyclin E1 protein expression

Given the discordance between amplification and protein expression in many TCGA samples, we sought to independently validate the data. To this end, we analyzed a TMA containing 140 primary HGSOC samples by FISH ( $n = 87$  informative cases) and IHC ( $n = 138$  informative cases).

In the FISH analysis, 23 cases (26.4%) showed *CCNE1* amplification, 34 cases (39.1%) showed relative *CCNE1* gain, and 30 cases (34.5%) were disomic for chromosome 19 (Fig. 2A). FISH classification criteria are described in Materials and Methods. In IHC analysis, protein expression was scored on a scale of 0 to 4 according to the percentage of immunopositive tumor cells present (Fig. 2B). For statistical analysis, scores 0 to 2 ( $<50\%$  positive cells) were considered "low expression" and scores 3 to 4 ( $>50\%$  positive cells) were considered "high expression." Using this scale, 38 cases (27.5%) were identified as high cyclin E1 expressors (Fig. 2B). Integration of FISH and IHC data revealed a significant difference in protein levels among cases with amplification, relative gain, or disomy ( $P = 0.0110$ ,  $\chi^2$  test; Fig. 2C). Twelve of 22 *CCNE1*-amplified cases (54.5%) were high expressors, a significantly higher proportion than in the

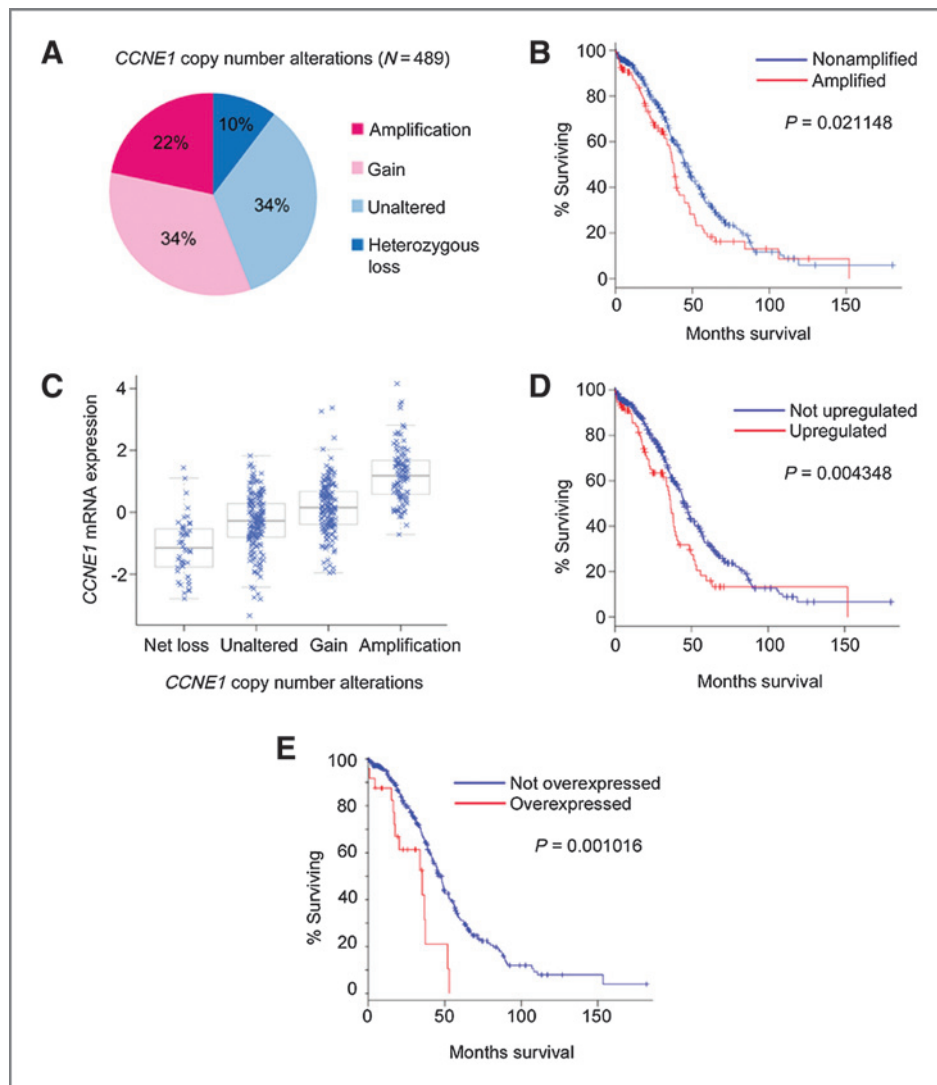


**Figure 1.** *CCNE1* alterations in HGSOc. A, distribution of somatic *CCNE1* copy number alterations across 489 tumors. B, reduced overall 5-year survival for patients with *CCNE1* amplifications. C, relationship between *CCNE1* copy number and mRNA expression. D and E, reduced overall 5-year survival for patients with elevated *CCNE1* mRNA (D) or overexpression of cyclin E1 protein (E;  $Z > 1.5$ ).

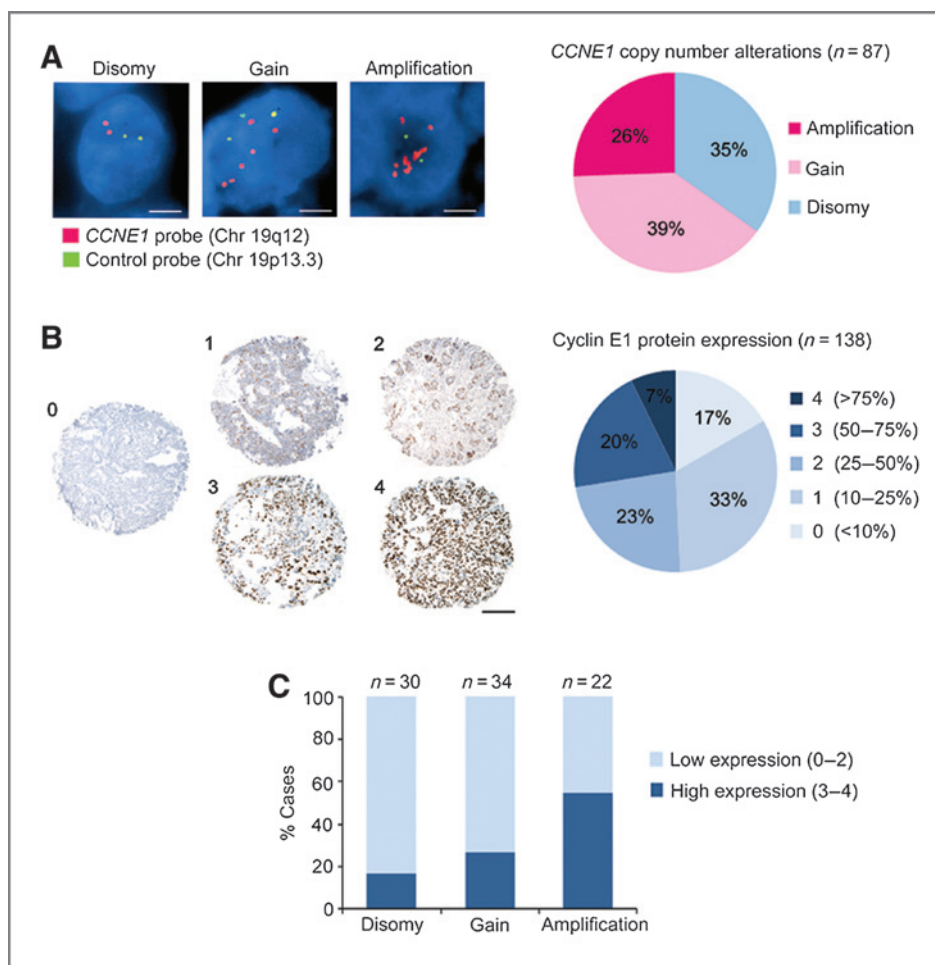
TCGA dataset. Conversely, 12 of 26 high expressers (46.2%) were *CCNE1* amplified. These data suggest that *CCNE1* amplification is linked to high protein expression in 46% to 55% of HGSOc cases.

#### Cyclin E1 overexpression occurs early in serous tumorigenesis

Although *CCNE1* amplifications are present in late-stage HGSOc, it remains unclear whether *CCNE1* deregulation contributes to early-stage tumor development. Given that tissue-targeted cyclin E1 expression induces mammary and lung carcinogenesis in mice (26–28), we hypothesized that early *CCNE1* aberrations may similarly drive HGSOc development. As previously mentioned, HGSOc likely arises from fallopian tube epithelium. We therefore asked whether cyclin E1 is expressed in early serous lesions of the fallopian tube. We analyzed fallopian tube specimens from 14 patients clinically diagnosed with high-grade serous adenocarcinoma of the ovary or fallopian tube, containing lesions that spanned the morphologic continuum from normal epithelium to invasive

carcinoma (Fig. 3A). This included putative precursor lesions called "p53 signatures" and noninvasive tumors termed as STIC. p53 signatures are stretches of secretory epithelial cells that exhibit intense p53 immunoreactivity but seem morphologically normal and have low proliferative activity (<10% Ki-67-positive nuclei; Fig. 3B; refs. 3, 16). p53 signatures have been shown to harbor DNA damage and somatic *TP53* mutations that result in p53 nuclear accumulation (3). STICs are noninvasive lesions characterized by nuclear atypia, loss of polarity, increased nuclear/cytoplasmic ratio, and high proliferative activity (>50% Ki-67-positive nuclei; Fig. 3C and D; refs. 29–32). STICs also harbor somatic *TP53* mutations and are usually p53-positive, although truncating mutations can result in loss of p53 immunoreactivity. It is hypothesized that p53 signatures are a normal physiologic entity possibly caused by damaging ovulatory factors, and that additional oncogenic events are required for p53 signatures to progress to STIC. p53-positive lesions exhibiting features intermediate between a p53 signature and STIC have been called TILTs (17). TILTs are also hypothesized to be precursors of STIC and we have grouped

**Figure 2.** *CCNE1* amplification is associated with increased cyclin E1 protein expression. A and B, a TMA containing 140 cases of primary HGSOC was analyzed by FISH and IHC to determine gene copy number and protein expression level, respectively. A, dual-color FISH analysis using a *CCNE1* probe (red) and chromosome 19 reference probe (green). Nuclei were counterstained with DAPI (blue). The graph represents distribution of *CCNE1* copy number alterations across 87 cases. Scale bar, 5  $\mu$ m. B, IHC analysis of cyclin E1 expression. The percentage of immunoreactive tumor cells (brown) was scored on a scale of 0 to 4. The graph shows the distribution of expression scores across 138 cases. Scale bar, 100  $\mu$ m. C, integration of FISH and IHC data shows that cyclin E1 expression is significantly higher in *CCNE1*-amplified cases ( $P = 0.0110$ ,  $\chi^2$  test).



them with p53 signatures in our analysis. By immunostaining serial tissue sections for p53, Ki-67, and cyclin E1, we identified precursor lesions (p53 signature/TILT) in 9 cases and STIC in 13 cases (Table 1). Normal tubal epithelium was present in 11 cases. Cyclin E1 expression in each lesion was scored as negative (<10% positive nuclei), low (10%–50% positive nuclei), or high (>50% positive nuclei). We found that although cyclin E1 was consistently absent in normal tubal epithelium, 3 out of 9 putative precursor lesions (33%) were cyclin E1-positive (Table 1). As shown in Fig. 3B, cyclin E1-positive cells outnumbered Ki-67-positive cells in the precursor lesions, indicating that cyclin E1 expression was not simply a read out of proliferation. Our data show that cyclin E1 overexpression can occur very early, even before STIC development, suggesting that deregulated *CCNE1* might cooperate with mutant p53 to drive tumorigenesis. Several studies have demonstrated oncogenic synergism between cyclin E1 and p53 defects, both *in vitro* and *in vivo* (10, 11, 28). Of the 13 STIC cases we analyzed, cyclin E1 expression was high in 7 cases (54%), low in 2 cases (15%), and absent in 4 cases (31%; Fig. 3C and D and Table 1). This suggests that only a subset of STICs exhibit high-level cyclin E1 expression and they may represent a distinct group of patients in whom *CCNE1* deregulation drives early-stage tumor progression.

### Constitutive cyclin E1 expression drives overproliferation of FTSECs

To understand how cyclin E1 might transform normal or p53-compromised secretory cells in the fallopian tube epithelium, we developed an *in vitro* model of cyclin E1-mediated transformation using primary human cells. Secretory epithelial cells were enzymatically dissociated from the fimbrial region of a fallopian tube tissue sample and cultured *in vitro* using methods recently described (18, 19). The cells were promptly transduced with *TERT* to delay replicative senescence. Next, we tried transducing TERT-expressing cells with *CCNE1*, but it did not enhance their growth and they underwent senescence within 2 passages (data not shown), likely reflecting a p53-mediated response to excess cyclin E1, as seen in other primary cell types (10, 33). To circumvent this outcome, we instead transduced TERT-expressing cells with mutant *TP53*<sup>R175H</sup>, one of the most common mutations found in p53 signatures, STIC, and HGSOC (3, 5). p53<sup>R175H</sup> is a conformational mutant that exerts a dominant negative effect by hetero-oligomerizing with wild-type p53, thus compromising its ability to transactivate target genes (34). p53<sup>R175H</sup> might also have gain-of-function oncogenic properties (34). Given that *TP53* is often somatically mutated at the precursor stage, we reasoned that *CCNE1* deregulation is likely to occur in the presence of mutant

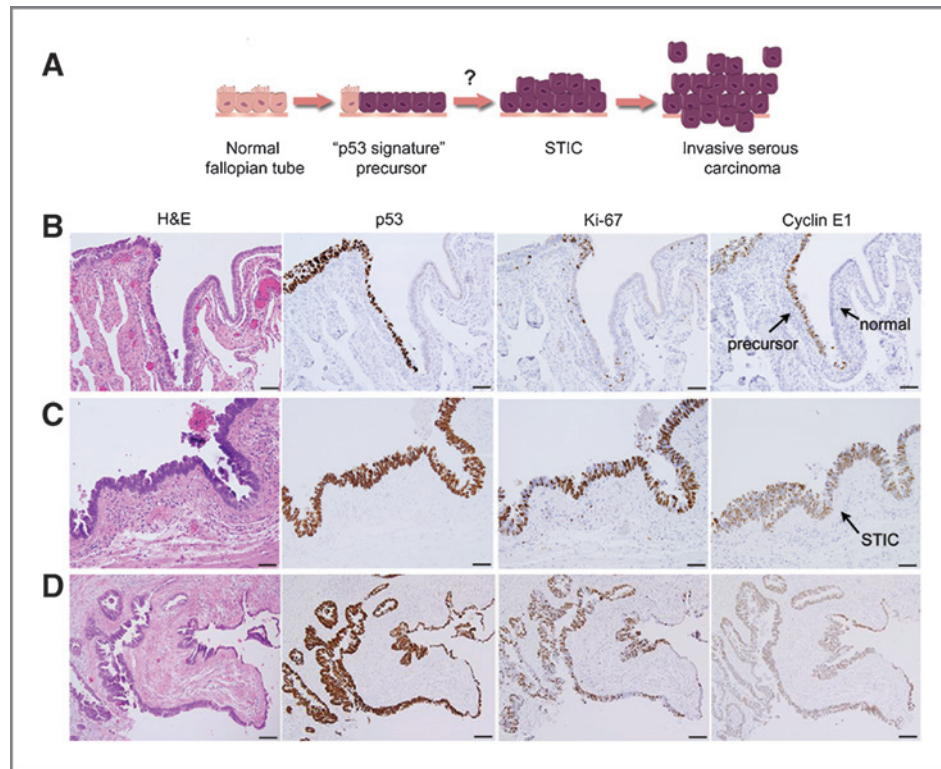


**Figure 3.** Cyclin E1 expression occurs early during serous tumorigenesis. A, an illustration of the proposed carcinogenic sequence for serous tumorigenesis in the fallopian tube epithelium. The "p53 signature" is hypothesized to precede STIC development. B, example of high cyclin E1 expression in a putative precursor lesion. Precursor cells are differentiated from adjacent normal cells by their nuclear p53 expression (brown), typically indicating somatic mutation of *TP53*. Note that cyclin E1 is expressed in precursor cells but not in adjacent normal cells. The proliferation marker Ki-67 is absent in most precursor cells, indicating low proliferative activity. Hematoxylin and eosin staining highlights histologic features. C and D, example of high cyclin E1 expression in STIC, shown at high (C) and low (D) magnifications. STICs are highly proliferative, indicated by high Ki-67 expression, and typically express mutant p53. STICs usually exhibit nuclear atypia and loss of polarity, evident by hematoxylin and eosin staining. Scale bars, 20  $\mu$ m (B and C), 50  $\mu$ m (D).

p53. Therefore, using *TP53*<sup>R175H</sup> to immortalize FTSECs is both physiologically relevant and chronologically accurate. FTSECs coexpressing TERT and p53<sup>R175H</sup> grew slowly but were proliferative enough to be expanded into a cell line, designated "FT282."

To characterize the effects of constitutive cyclin E1 expression on p53-compromised but untransformed cells, we transduced FT282 cells with either *CCNE1* or an empty vector control. The resulting cell lines were designated "FT282-CCNE1" and "FT282-V," respectively. Western blot analysis was used to validate exogenous gene expression (cyclin E1, p53) and to verify the expression of appropriate Müllerian

lineage markers, namely paired box 8 (PAX8) and cytokeratin-7 (CK7; Fig. 4A). Cyclin E1 overexpression triggered phosphorylation of its binding partner CDK2 on Thr160, indicating CDK2 activation (Fig. 4A; ref. 35). Accordingly, FT282-CCNE1 cells exhibited accelerated growth in SRB proliferation assays (Fig. 4B). FT282-CCNE1 cell density increased by 4.45-fold ( $\pm 0.96$  SD) over 72 hours, whereas FT282-V cell density increased by only 1.61-fold ( $\pm 0.27$  SD;  $P = 1.14 \times 10^{-11}$ , Student *t* test; Fig. 4B). When seeded sparsely in clonogenic assays, FT282-CCNE1 cells exhibited clonal growth, whereas FT282-V cells typically remained as single cells, often appearing senescent (Fig. 4C). When seeded at moderate density ( $\sim 50\%$ ),

**Table 1.** Cyclin E1 expression in early-stage serous lesions of the fallopian tube

|                                   | Negative<br>(<10% pos nuclei; %) | Low<br>(10%–50% pos nuclei; %) | High<br>(>50% pos nuclei; %) |
|-----------------------------------|----------------------------------|--------------------------------|------------------------------|
| Total cases, $N = 14$             |                                  |                                |                              |
| Normal FTE ( $n = 11$ )           | 11/11 (100)                      | 0/11 (0)                       | 0/11 (0)                     |
| p53 signature or TILT ( $n = 9$ ) | 6/9 (66)                         | 0/9 (0)                        | 3/9 (33)                     |
| STIC ( $n = 13$ )                 | 4/13 (31)                        | 2/13 (15)                      | 7/13 (54)                    |

Abbreviations: FTE, fallopian tube epithelium; TILT, tubal intraepithelial lesion in transition; STIC, serous tubal intraepithelial carcinoma.

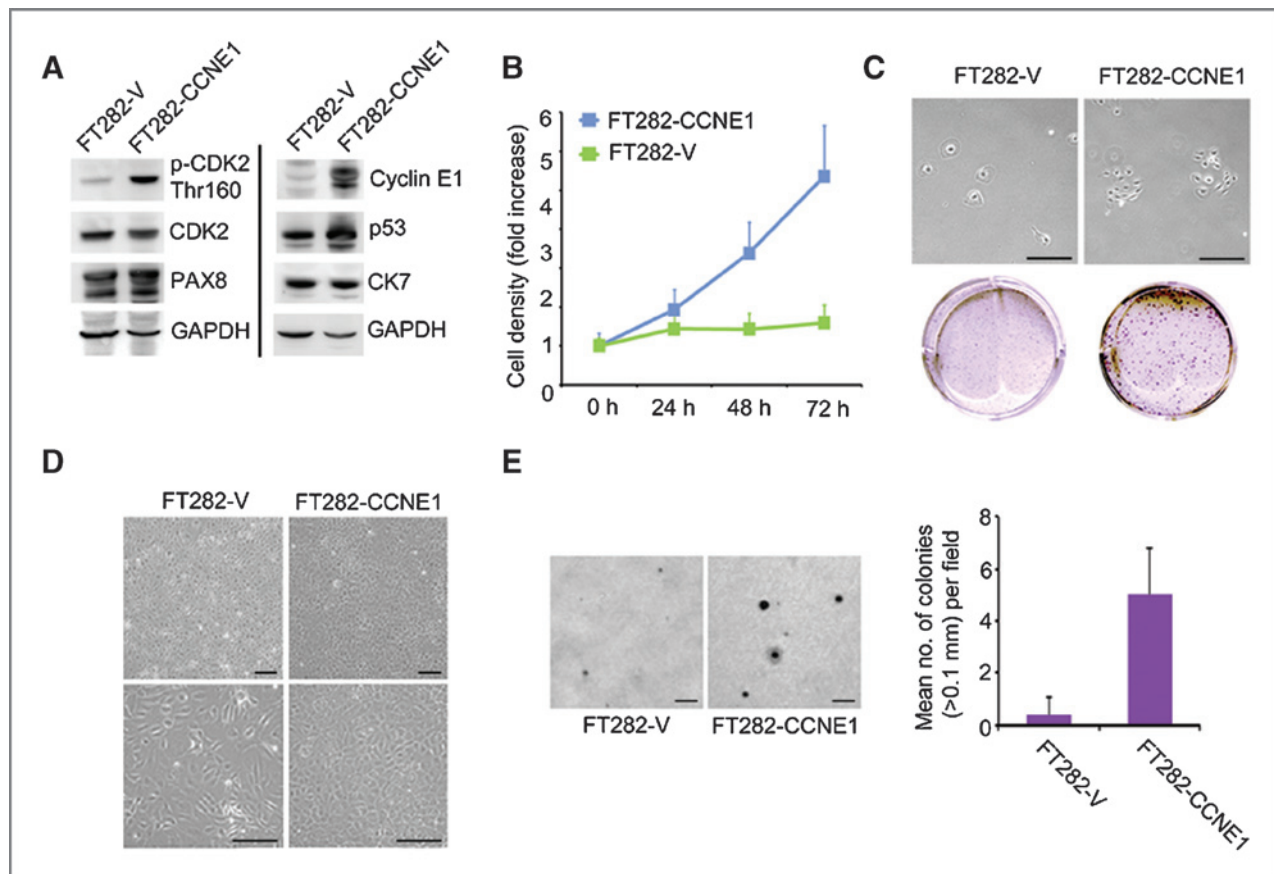


**Figure 4.** Constitutive cyclin E1 expression leads to uncontrolled growth of immortal FTSECs. A, primary human FTSECs immortalized with *TERT* and *TP53<sup>R175H</sup>* were transduced with *CCNE1* (FT282-CCNE1) or empty vector (FT282-V). Western blot analysis was used to validate expression of cyclin E1, p53, and endogenous Müllerian lineage markers (PAX8, CK7). Phospho-CDK2-Thr160 indicates CDK2 activation. A composite blot is shown; samples were loaded in duplicate to accommodate numerous antibody incubations. Full-length blots are presented in Supplementary Figure S1. B, constitutive expression of cyclin E1 increased cell proliferation rate ( $P = 1.14 \times 10^{-11}$  at  $t = 72$  hours, Student  $t$  test). C, cyclin E1 expression also promoted clonogenic growth. Top, shows cells in culture; bottom, shows cells fixed and stained with crystal violet. D, cyclin E1 induced the loss of contact inhibition, resulting in overcrowded cell culture. Images depict confluent cells at low (top) and high (bottom) magnification. E, cyclin E1 promoted subtle anchorage-independent colony formation in soft agar ( $P = 4.47 \times 10^{-7}$ , Student  $t$  test). Error bars represent SD. Scale bars, 50  $\mu\text{m}$  (C and D), 500  $\mu\text{m}$  (E).

FT282-V cells grew to 90% to 100% confluency and thereafter could be maintained as contact-inhibited monolayers for weeks. Conversely, FT282-CCNE1 cells continued to divide when confluent and quickly became overcrowded, indicating loss of contact inhibition (Fig. 4D). Tightly packed FT282-CCNE1 cultures remained viable, however, showing no evidence of stress-induced apoptosis. Finally, cyclin E1 overexpression induced a small but significant degree of anchorage-independent growth, evidenced by colony formation in soft agar. Although FT282-V cells produced virtually no colonies (0.4 colonies per field  $\pm 0.70$  SD), FT282-CCNE1 cells formed small, slow-growing colonies (5 colonies per field  $\pm 1.76$  SD;  $P = 4.47 \times 10^{-7}$ , Student  $t$  test; Fig. 4E). Loss of contact inhibition and anchorage-independent growth by FT282-CCNE1 cells emerged at mid-passage number ( $\sim p20$ ). FT282-V cells at equivalent passage number did not exhibit a similar phenotype. These data suggest that *TP53* mutation alone does not drive FTSEC proliferation but rather impairs the  $G_1$ -S checkpoint such that growth arrest cannot be executed in response to *CCNE1* deregulation. Under these

conditions, cyclin E1 readily drives inappropriate cell growth.

#### Constitutive cyclin E1 expression causes DNA damage in FTSECs

Recent studies suggest that deregulated *CCNE1* induces genomic instability by generating DNA replication stress (36, 37). Replication stress, broadly defined as inefficient DNA replication, is caused by impediments to replication fork progression, for example, obstructive DNA lesions, replication inhibitors, or depletion of components required for DNA synthesis. Stalled replication forks are dangerous because they can collapse into DSBs. The mechanism by which cyclin E1 generates replication stress is not completely clear. It was reported that deregulated *CCNE1* forces S-phase entry without adequate nucleotide pools, resulting in incomplete DNA replication and fork collapse (36). Cyclin E1 overexpression has also been shown to cause excessive origin firing, which increases the number of active replication forks and creates spatial conflicts between replication and transcription

machineries (37). To determine whether cyclin E1 overexpression induced DNA damage in our model, we analyzed cells for the presence of  $\gamma$ -H2AX (p-H2A.X Ser139) nuclear foci by immunofluorescent staining. H2AX is a histone protein phosphorylated by ataxia telangiectasia mutated (ATM) or ataxia telangiectasia and Rad3 related (ATR) at sites of DNA damage. It is predominantly phosphorylated by ATM at DSBs (38). We detected prominent  $\gamma$ -H2AX foci in 27.2% ( $\pm 7.6\%$  SD) of FT282-CCNE1 nuclei compared with only 8.0% ( $\pm 3.1\%$  SD) of FT282-V nuclei, representing an approximate 3.4-fold increase in DSBs ( $P = 0.0035$ , Student *t* test; Fig. 5A). Because H2AX can also be phosphorylated by ATR at single-strand breaks (SSB; ref. 38), we looked for evidence of SSBs using the Comet assay, in which

migration of damaged DNA gives the appearance of a comet "tail" in single-cell gel electrophoresis (39). We found a significantly higher proportion of DNA in the tails of FT282-CCNE1 cells (5.09%  $\pm 5.09\%$  SD) compared with FT282-V cells (3.04%  $\pm 3.37\%$  SD), representing a 1.67-fold increase in DNA damage ( $P = 0.000383$ , Student *t* test; Fig. 5B). It should be noted that active replication forks appear as SSBs in the Comet assay. Therefore, the increase in DNA damage could represent stalled or lagging replication forks, consistent with replication stress.

Finally, we asked whether cyclin E1-induced DNA damage would alter the regulation of DDR genes. Using quantitative PCR array profiling, we analyzed the expression of 84 DDR-related genes and identified 14 genes differentially expressed in

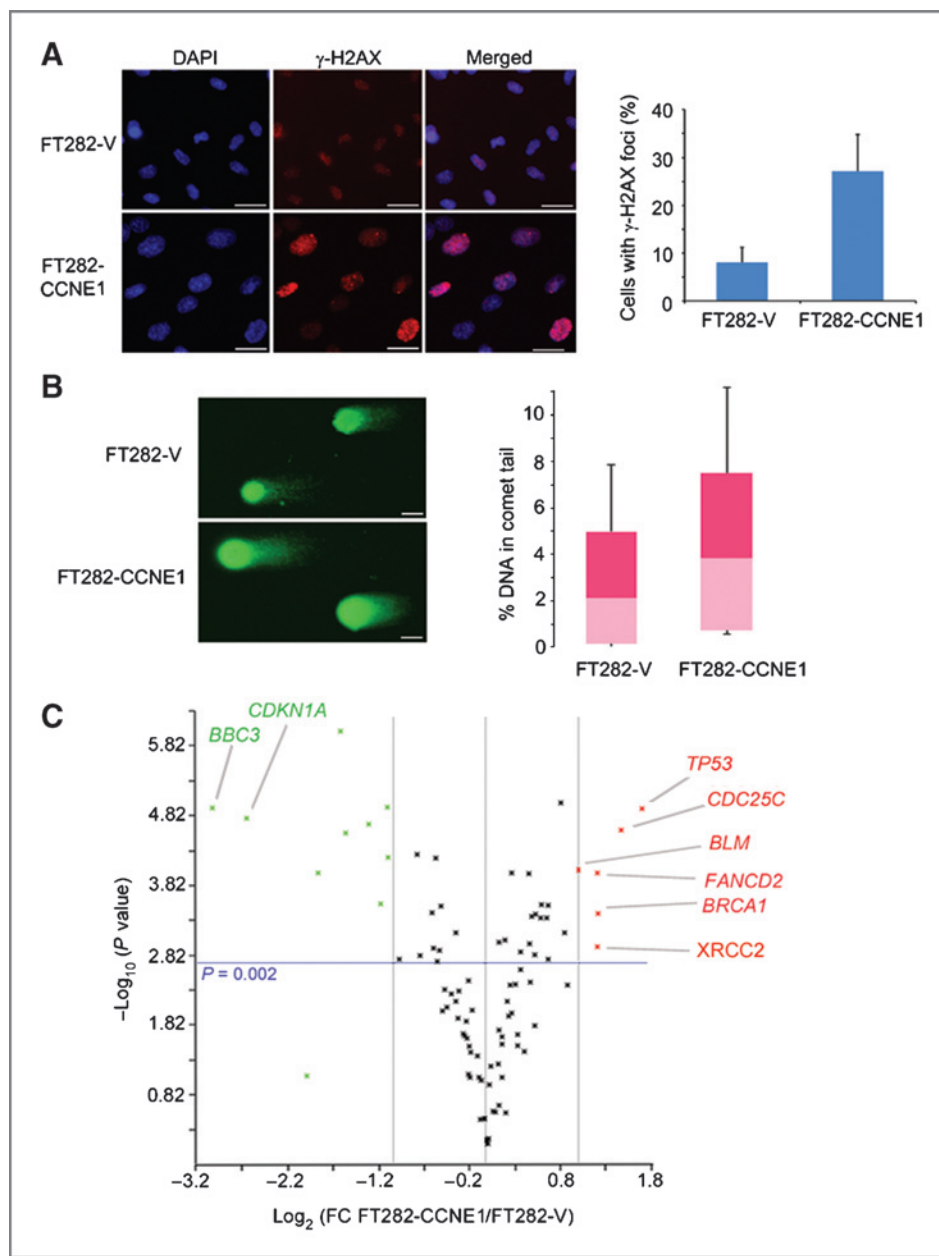


**Figure 5.** Cyclin E1 expression leads to DNA damage in immortal FTSECs. **A**, immunofluorescent staining of  $\gamma$ -H2AX nuclear foci at sites of DNA DSBs (red dots). Nuclei were counterstained with DAPI (blue). Cyclin E1-overexpressing cells had significantly more  $\gamma$ -H2AX foci than control cells ( $P = 0.0035$ , Student *t* test). Graph shows quantification of foci ( $\pm$ SD). **B**, Comet assay for DNA damage. Comet "tails" represent DNA with single strand or DSBs. Cyclin E1-overexpressing cells had a greater proportion of DNA in "tails" than did control cells, indicating increased DNA damage ( $P = 0.000383$ , Student *t* test). The box plot shows the range of percentage tail DNA per cell. Scale bars, 50  $\mu$ m (**A** and **B**). **C**, expression of 84 DDR genes in cyclin E1-overexpressing cells compared with vector controls, measured by quantitative PCR array. Volcano plot shows genes upregulated (red) or downregulated (green) by  $>2$ -fold ( $P < 0.002$ ). Fold-change values are presented in Table 2 and Supplementary Table S2.

**Table 2.** DDR genes up- or downregulated in FT282-CCNE1 cells relative to FT282-V cells

| Gene symbol    | Fold-regulation | P <sup>a</sup> |
|----------------|-----------------|----------------|
| <i>TP53</i>    | 3.2583          | 0.000012       |
| <i>CDC25C</i>  | 2.7845          | 0.000025       |
| <i>BRCA1</i>   | 2.3415          | 0.000391       |
| <i>FANCD2</i>  | 2.3307          | 0.000101       |
| <i>XRCC2</i>   | 2.3307          | 0.001179       |
| <i>BLM</i>     | 2.0150          | 0.000093       |
| <i>BAX</i>     | -2.0838         | 0.000061       |
| <i>MAPK12</i>  | -2.0935         | 0.000012       |
| <i>GADD45G</i> | -2.2026         | 0.000285       |
| <i>DDB2</i>    | -2.4103         | 0.000020       |
| <i>B2M</i>     | -2.8664         | 0.000027       |
| <i>MPG</i>     | -2.9812         | 0.000001       |
| <i>ATM</i>     | -3.5208         | 0.000101       |
| <i>CDKN1A</i>  | -6.0317         | 0.000017       |
| <i>BBC3</i>    | -7.8312         | 0.000012       |

<sup>a</sup>P values were calculated based on Student *t* tests of the triplicate  $2^{(-\Delta C_t)}$  values for each target gene in the control (FT282-V) and treatment (FT282-CCNE1) groups.

FT282-CCNE1 cells compared with FT282-V cells (>2-fold difference,  $P < 0.002$ , Student *t* test; Fig. 5C and Supplementary Table S2). Upregulated genes included *TP53*, *CDC25C*, *BRCA1*, *FANCD2*, *XRCC2*, and *BLM* (Table 2). Downregulated genes included *BBC3*, *CDKN1A*, *ATM*, *MPG*, *B2M*, *DDB2*, *GADD45G*, *MAPK12*, and *BAX*. Although *TP53* was upregulated (+3.3-fold), it failed to transactivate its transcriptional targets, *CDKN1A* (p21<sup>CIP1</sup>) and *BBC3* (Puma), consistent with the exertion of a dominant negative effect by ectopic p53<sup>R175H</sup>. P21<sup>CIP1</sup> and Puma are key effectors of p53-induced cell-cycle arrest and apoptosis, respectively (34). *CDKN1A* and *BBC3* were downregulated (-6.0- and -7.8-fold), suggesting that constitutive cyclin E1 expression might repress these genes. Other alterations that would promote cell viability and proliferation included upregulation of *CDC25C* (+2.78), which promotes mitotic entry; downregulation of proapoptotic *BAX* (-2.08), downregulation of *GADD45G* (-2.20), which induces growth arrest after DNA damage, and downregulation of *MAPK12* (-2.09), a stress-activated negative regulator of cell-cycle progression. These results are consistent with our observation that confluent FT282-CCNE1 cells continue to proliferate and exhibit no apoptosis (Fig. 4D). Most of the genes found upregulated (*BRCA1*, *FANCD2*, *BLM*, *XRCC2*) are directly involved in DNA damage repair, suggesting that cyclin E1 overexpression may prompt the cell to increase its DNA repair capacity by upregulating key repair factors.

## Discussion

The molecular pathogenesis of HGSOC remains poorly understood, and oncogenic drivers of this cancer must be identified to guide novel therapeutic approaches. In this study, we have characterized the oncogenic role of *CCNE1* in HGSOC

development and provided evidence that *CCNE1* deregulation may contribute to serous tumorigenesis and chromosomal instability in the fallopian tube.

First, we identified cases in the TCGA database with somatic *CCNE1* gene amplification, mRNA upregulation, and/or protein overexpression, and showed that each alteration type is associated with reduced overall survival. This finding suggests that deregulated *CCNE1* is an oncogenic driver of late-stage HGSOC progression when amplified, transcriptionally upregulated, or overexpressed, although reduced survival rates may also reflect resistance to platinum-based chemotherapy, previously found to be associated with the *CCNE1* amplicon (13, 14). Using FISH and IHC analysis, we showed that *CCNE1* amplifications lead to high-level cyclin E1 protein expression in >50% of cases. In agreement with our results, two studies have reported correlations among *CCNE1* amplification, cyclin E1 expression, and reduced survival in ovarian cancer (14, 24). However, one of them included multiple tumor subtypes in their analysis. Because there is now strong evidence that HGSOC pathogenesis differs dramatically from that of other subtypes (40), we restricted our study to high-grade serous tumors only, thus eliminating the possibility of subtype-specific confounding factors.

Second, we showed that *CCNE1* deregulation might promote serous tumorigenesis within the fallopian tube epithelium. IHC analysis of fallopian tubes from patients with HGSOC revealed cyclin E1 overexpression in a subset of putative precursors and noninvasive lesions, thus implicating cyclin E1 at the earliest stages of tumor development. A recent study examining cyclin E1 expression in the fallopian tubes of 23 patients with HGSOC noted a cyclin E1-positive precursor in one case (41). Our data bolster that finding and provide additional evidence for *CCNE1* deregulation at the precursor stage. It has been reported that cyclin E1 is present in a majority of STICs, although expression levels varied considerably (3, 41). Sehdev and colleagues found that cyclin E1 was expressed in 24 of 35 STICs (69%) collected from 22 patients (41). However, only 16 (46%) of those STICs exhibited high expression (>50% positive cells). We propose that high-level cyclin E1 expression could highlight specific cases in which tumor development is driven by *CCNE1* deregulation as opposed to other oncogenic mechanisms. Given that *TP53* mutations are present in nearly all STICs and many putative precursors (3, 31), p53 dysfunction is likely required for cyclin E1-driven tumorigenesis in the fallopian tube. It has been shown that excess cyclin E1 triggers a DDR, causing p53 stabilization and activation (42). Activated p53 rapidly intervenes by transcriptionally upregulating the cyclin E1/CDK2 inhibitor *CDKN1A* (p21<sup>CIP1</sup>), which shuts down CDK2 activity and mediates cell-cycle arrest. If p21 is disabled, p53 will instead activate apoptosis through alternate mediators to mitigate the effects of cyclin E1. Thus, p53 must be mutated (or otherwise inactivated) for the cell to tolerate *CCNE1* deregulation (42). Although our data support the hypothesis that *CCNE1* deregulation is an early event, the causes of *CCNE1* deregulation in the fallopian tube epithelium remain ill defined. Gene amplification is one possibility; two studies reported

recurrent *CCNE1* copy number gains/amplifications in early-stage (FIGO stage I–II) fallopian tube carcinomas (43, 44). However, given that >40% of our cyclin E1–overexpressing TMA samples lacked amplification (Fig. 2C), additional mechanisms of *CCNE1* upregulation must be at play, possibly transcriptional activation by other oncogenes or decreased ubiquitin-mediated degradation (8).

Third, after observing cyclin E1 expression in early tubal lesions, we created a model of cyclin E1–mediated transformation using primary human FTSECs. The cells were immortalized in a physiologically relevant manner by introducing a form of mutant p53 (*TP53*<sup>R175H</sup>) that is found in both p53 signatures and STICs (3, 31). Through a series of *in vitro* assays, we demonstrated that constitutive cyclin E1 expression induces overproliferation of p53-compromised FTSECs and the acquisition of malignant characteristics such as clonal growth ability, loss of contact inhibition, and colony formation in soft agar. It should be noted that cyclin E1 overexpression did not result in an aggressively malignant phenotype, like that seen with H-RAS<sup>V12</sup> or c-MYC (19), suggesting that additional genetic events are required for full transformation. To determine what those might be, we are currently screening genes that are coamplified or coexpressed with *CCNE1* in HGSOE [for example, *TPX2* (14)] for their ability to transform FTSECs. Alternatively, cyclin E1 might require cleavage to reach its full oncogenic potential. A number of studies have shown that low molecular weight forms of cyclin E1, produced by elastase-mediated cleavage, cause genomic instability and promote aggressive tumor phenotypes in breast cancer (45, 46). It has also been reported that the chromatin remodeling protein Rsf-1 (remodeling and spacing factor 1) is coexpressed with cyclin E1 in HGSOE and that Rsf-1/cyclin E1 complexes promote the transformation of immortalized rat kidney cells expressing mutant p53<sup>R175H</sup> (47). Interestingly, Rsf-1/cyclin E1 complexes required p53<sup>R175H</sup> to induce tumorigenicity and could not transform p53 wild-type cells, again underscoring the importance of mutant p53 in cyclin E1–mediated tumorigenesis.

Finally, we demonstrated that cyclin E1 overexpression in FTSECs causes DNA damage and alters the expression of DDR genes. Multiple negative cell-cycle regulators that are normally activated by DNA damage were downregulated. Meanwhile, specific DNA repair genes were upregulated, including *BRCA1*, *FANCD2*, *XRCC2*, and *BLM*. Interestingly, these genes are central components of a "fork protection pathway" that protects stalled DNA replication forks from degradation and facilitates fork recovery. Schlacher and colleagues have shown that monoubiquitinated FANCD2 (Fanconi anemia, complementation group D2) complexes with BRCA1 to stabilize stalled forks (48). Chaudhury and colleagues additionally

reported that FANCD2 is a critical regulator of Bloom syndrome, RecQ helicase-like (BLM) helicase activity and that the two proteins act in concert to restart stalled replication forks (49). XRCC2 is a RAD51 paralog that complexes with RAD51C, another key fork stabilization factor (48). Upregulation of these genes possibly enables cells to manage high levels of replication stress brought on by *CCNE1* deregulation. Upregulation of *BRCA1* is notable given the rarity of *CCNE1* amplification in *BRCA1*-mutated HGSOE. *CCNE1*-amplified tumors might depend on BRCA1 to mitigate replication stress and thus maintain cell viability in the face of accumulating chromosomal instability.

In summary, our data support a model whereby *CCNE1* deregulation drives uncontrolled growth of FTSECs harboring somatic *TP53* defects and causes DNA damage by inducing replication stress, thus generating chromosomal instability and promoting tumorigenesis.

#### Disclosure of Potential Conflicts of Interest

No potential conflicts of interest were disclosed.

#### Authors' Contributions

**Conception and design:** A.M. Karst, R. Drapkin

**Development of methodology:** A.M. Karst, P.M. Jones

**Acquisition of data (provided animals, acquired and managed patients, provided facilities, etc.):** A.M. Karst, P.M. Jones, N. Vena, J.F. Liu, M.S. Hirsch, D.D.L. Bowtell

**Analysis and interpretation of data (e.g., statistical analysis, biostatistics, computational analysis):** A.M. Karst, P.M. Jones, A.H. Ligon, J.F. Liu, D.D.L. Bowtell, R. Drapkin

**Writing, review, and/or revision of the manuscript:** A.M. Karst, A.H. Ligon, D. Etemadmoghadam, D.D.L. Bowtell, R. Drapkin

**Administrative, technical, or material support (i.e., reporting or organizing data, constructing databases):** P.M. Jones, M.S. Hirsch

**Study supervision:** R. Drapkin

#### Acknowledgments

The authors thank the BWH Department of Pathology faculty and staff for allocation of tissues and members of the Drapkin and Bowtell laboratories for fruitful discussions.

#### Grant Support

This work was supported by grants from the National Cancer Institute at the NIH P50-CA105009 (R. Drapkin), NIH U01 CA-152990 (R. Drapkin), NIH R21 CA-156021 (R. Drapkin); the Honorable Tina Brozman 'Tina's Wish' Foundation (R. Drapkin), the Dr. Miriam and Sheldon G. Adelson Medical Research Foundation (R. Drapkin), the Robert and Debra First Fund (R. Drapkin), the Gamel Family Fund (R. Drapkin), a Canadian Institutes of Health Research Fellowship (A.M. Karst), a Kaleidoscope of Hope Foundation Young Investigator Research Grant (A.M. Karst), and a National Health and Medical Research Council project grant (APP 1042358; D.D.L. Bowtell).

The costs of publication of this article were defrayed in part by the payment of page charges. This article must therefore be hereby marked *advertisement* in accordance with 18 U.S.C. Section 1734 solely to indicate this fact.

Received August 8, 2013; revised November 18, 2013; accepted November 20, 2013; published OnlineFirst December 23, 2013.

#### References

- Peter Boyle, Bernard Levin, editors. World cancer report 2008. Geneva: International Agency for Research on Cancer; 2008.
- Nik NN, Vang R, Shih IM, Kurman RJ. Origin and pathogenesis of pelvic (ovarian, tubal, and primary peritoneal) serous carcinoma. *Annu Rev Pathol* 2013;16:27–45.
- Lee Y, Miron A, Drapkin R, Nucci MR, Medeiros F, Saleemuddin A, et al. A candidate precursor to serous carcinoma that originates in the distal fallopian tube. *J Pathol* 2007;211:26–35.
- Dubeau L, Drapkin R. Coming into focus: the nonovarian origins of ovarian cancer. *Ann Oncol* 2013;24 Suppl 8:viii28–viii35.

5. TCGA. Integrated genomic analyses of ovarian carcinoma. *Nature* 2011;474:609–15.
6. Goringe KL, George J, Anglesio MS, Ramakrishna M, Etemadmoghadam D, Cowin P, et al. Copy number analysis identifies novel interactions between genomic loci in ovarian cancer. *PLoS ONE* 2010; 5:e11408
7. Bowtell DD. The genesis and evolution of high-grade serous ovarian cancer. *Nat Rev Cancer* 2010;10:803–8.
8. Siu KT, Rosner MR, Minella AC. An integrated view of cyclin E function and regulation. *Cell Cycle* 2012;11:57–64.
9. Spruck CH, Won KA, Reed SI. Deregulated cyclin E induces chromosome instability. *Nature* 1999;401:297–300.
10. Minella AC, Swanger J, Bryant E, Welcker M, Hwang H, Clurman BE. p53 and p21 form an inducible barrier that protects cells against cyclin E-cdk2 deregulation. *Curr Biol* 2002;12:1817–27.
11. Loeb KR, Kostner H, Firpo E, Norwood T, D Tsuchiya K, Clurman BE, et al. A mouse model for cyclin E-dependent genetic instability and tumorigenesis. *Cancer Cell* 2005;8:35–47.
12. Engler DA, Gupta S, Growdon WB, Drapkin RI, Nitta M, Sargent PA, et al. Genome wide DNA copy number analysis of serous type ovarian carcinomas identifies genetic markers predictive of clinical outcome. *PLoS ONE* 2012;7:e30996.
13. Etemadmoghadam D, deFazio A, Beroukhir R, Mermel C, George J, Getz G, et al. Integrated genome-wide DNA copy number and expression analysis identifies distinct mechanisms of primary chemoresistance in ovarian carcinomas. *Clin Cancer Res* 2009;15: 1417–27.
14. Etemadmoghadam D, George J, Cowin PA, Cullinane C, Kansara M, Goringe KL, et al. Amplicon-dependent CCNE1 expression is critical for clonogenic survival after cisplatin treatment and is correlated with 20q11 gain in ovarian cancer. *PLoS ONE* 2010;5:e15498.
15. Liu JF, Hirsch MS, Lee H, Matulonis UA. Prognosis and hormone receptor status in older and younger patients with advanced-stage papillary serous ovarian carcinoma. *Gynecol Oncol* 2009;115:401–6.
16. Mehrad M, Ning G, Chen EY, Mehra KK, Crum CP. A pathologist's road map to benign, precancerous, and malignant intraepithelial proliferations in the fallopian tube. *Adv Anat Pathol* 2010;17:293–302.
17. Jarboe E, Folkins A, Nucci MR, Kindelberger D, Drapkin R, Miron A, et al. Serous carcinogenesis in the fallopian tube: a descriptive classification. *Int J Gynecol Pathol* 2008;27:1–9.
18. Karst AM, Drapkin R. Primary culture and immortalization of human fallopian tube secretory epithelial cells. *Nat Protoc* 2012;7:1755–64.
19. Karst AM, Levanon K, Drapkin R. Modeling high-grade serous ovarian carcinogenesis from the fallopian tube. *Proc Natl Acad Sci U S A* 2011; 108:7547–52.
20. Counter CM, Hahn WC, Wei W, Caddle SD, Beijersbergen RL, Lansford PM, et al. Dissociation among *in vitro* telomerase activity, telomere maintenance, and cellular immortalization. *Proc Natl Acad Sci U S A* 1998;95:14723–8.
21. Junk DJ, Vrba L, Watts GS, Oshiro MM, Martinez JD, Futscher BW. Different mutant/wild-type p53 combinations cause a spectrum of increased invasive potential in nonmalignant immortalized human mammary epithelial cells. *Neoplasia* 2008;10:450–61.
22. Cerami E, Gao J, Dogrusoz U, Gross BE, Sumer SO, Aksoy BA, et al. The cBio cancer genomics portal: an open platform for exploring multidimensional cancer genomics data. *Cancer Discov* 2012;2: 401–4.
23. Gao J, Aksoy BA, Dogrusoz U, Dresdner G, Gross B, Sumer SO, et al. Integrative analysis of complex cancer genomics and clinical profiles using the cBioPortal. *Sci Signal* 2013;6:pl1.
24. Nakayama N, Nakayama K, Shamima Y, Ishikawa M, Katagiri A, Iida K, et al. Gene amplification CCNE1 is related to poor survival and potential therapeutic target in ovarian cancer. *Cancer* 2010;116: 2621–34.
25. Ofir M, Hacohen D, Ginsberg D. MiR-15 and miR-16 are direct transcriptional targets of E2F1 that limit E2F-induced proliferation by targeting cyclin E. *Mol Cancer Res* 2011;9:440–7.
26. Bortner DM, Rosenberg MP. Induction of mammary gland hyperplasia and carcinomas in transgenic mice expressing human cyclin E. *Mol Cell Biol* 1997;17:453–9.
27. Ma Y, Fiering S, Black C, Liu X, Yuan Z, Memoli VA, et al. Transgenic cyclin E triggers dysplasia and multiple pulmonary adenocarcinomas. *Proc Natl Acad Sci U S A* 2007;104: 4089–94.
28. Smith AP, Henze M, Lee JA, Osborn KG, Keck JM, Tedesco D, et al. Deregulated cyclin E promotes p53 loss of heterozygosity and tumorigenesis in the mouse mammary gland. *Oncogene* 2006;25: 7245–59.
29. Piek JM, van Diest PJ, Zweemer RP, Jansen JW, Poort-Keesom RJ, Menko FH, et al. Dysplastic changes in prophylactically removed fallopian tubes of women predisposed to developing ovarian cancer. *J Pathol* 2001;195:451–6.
30. Paley PJ, Swisher EM, Garcia RL, Agoff SN, Greer BE, Peters KL, et al. Occult cancer of the fallopian tube in BRCA-1 germline mutation carriers at prophylactic oophorectomy: a case for recommending hysterectomy at surgical prophylaxis. *Gynecol Oncol* 2001;80:176–80.
31. Kindelberger DW, Lee Y, Miron A, Hirsch MS, Feltmate C, Medeiros F, et al. Intraepithelial carcinoma of the fimbria and pelvic serous carcinoma: evidence for a causal relationship. *Am J Surg Pathol* 2007; 31:161–9.
32. Medeiros F, Muto MG, Lee Y, Elvin JA, Callahan MJ, Feltmate C, et al. The tubal fimbria is a preferred site for early adenocarcinoma in women with familial ovarian cancer syndrome. *Am J Surg Pathol* 2006;30: 230–6.
33. Bartkova J, Rezaei N, Liontos M, Karakaidos P, Kletsas D, Issaeva N, et al. Oncogene-induced senescence is part of the tumorigenesis barrier imposed by DNA damage checkpoints. *Nature* 2006;444: 633–7.
34. Brosh R, Rotter V. When mutants gain new powers: news from the mutant p53 field. *Nat Rev Cancer* 2009;9:701–13.
35. Brown NR, Noble ME, Lawrie AM, Morris MC, Tunnah P, Divita G, et al. Effects of phosphorylation of threonine 160 on cyclin-dependent kinase 2 structure and activity. *J Biol Chem* 1999;274: 8746–56.
36. Bester AC, Roniger M, Oren YS, Im MM, Sarni D, Chaoat M, et al. Nucleotide deficiency promotes genomic instability in early stages of cancer development. *Cell* 2011;145:435–46.
37. Jones RM, Mortusewicz O, Afzal I, Lorvellec M, Garcia P, Helleday T, et al. Increased replication initiation and conflicts with transcription underlie cyclin E-induced replication stress. *Oncogene* 2013;32: 3744–53.
38. Podhorecka M, Skladanowski A, Bozko P. H2AX phosphorylation: its role in DNA damage response and cancer therapy. *J Nucleic Acids* 2010;pii: 920161.
39. Olive PL, Banath JP. The comet assay: a method to measure DNA damage in individual cells. *Nat Protoc* 2006;1:23–9.
40. Karst AM, Drapkin R. Ovarian cancer pathogenesis: a model in evolution. *J Oncol* 2010;2010:932371.
41. Sehdev AS, Kurman RJ, Kuhn E, Shih Ie M. Serous tubal intraepithelial carcinoma upregulates markers associated with high-grade serous carcinomas including Rsf-1 (HBXAP), cyclin E and fatty acid synthase. *Mod Pathol* 2010;23:844–55.
42. Minella AC, Grim JE, Welcker M, Clurman BE. p53 and SCFFbw7 cooperatively restrain cyclin E-associated genome instability. *Oncogene* 2007;26:6948–53.
43. Nowee ME, Snijders AM, Rockx DA, de Wit RM, Kosma VM, Hama-lainen K, et al. DNA profiling of primary serous ovarian and fallopian tube carcinomas with array comparative genomic hybridization and multiplex ligation-dependent probe amplification. *J Pathol* 2007;213: 46–55.
44. Snijders AM, Nowee ME, Fridlyand J, Piek JM, Dorsman JC, Jain AN, et al. Genome-wide-array-based comparative genomic hybridization reveals genetic homogeneity and frequent copy number increases encompassing CCNE1 in fallopian tube carcinoma. *Oncogene* 2003; 22:4281–6.
45. Bagheri-Yarmand R, Biernacka A, Hunt KK, Keyomarsi K. Low molecular weight cyclin E overexpression shortens mitosis, leading to chromosome missegregation and centrosome amplification. *Cancer Res* 2010;70:5074–84.

Karst et al.

---

46. Duong MT, Aki S, Wei C, Wingate HF, Liu W, Lu Y, et al. LMW-E/CDK2 deregulates acinar morphogenesis, induces tumorigenesis, and associates with the activated b-Raf-ERK1/2-mTOR pathway in breast cancer patients. *PLoS Genet* 2012;8:e1002538.
47. Sheu JJ, Choi JH, Guan B, Tsai FJ, Hua CH, Lai MT, et al. Rsf-1, a chromatin remodelling protein, interacts with cyclin E1 and promotes tumour development. *J Pathol* 2013;229:559–68.
48. Schlacher K, Wu H, Jasin M. A distinct replication fork protection pathway connects Fanconi anemia tumor suppressors to RAD51-BRCA1/2. *Cancer Cell* 2012;22:106–16.
49. Chaudhury I, Sareen A, Raghunandan M, Sobeck A. FANCD2 regulates BLM complex functions independently of FANCI to promote replication fork recovery. *Nucleic Acids Res* 2013;41:6444–59.